

# HIGHLY FLEXIBLE, TRANSPARENT AND PATTERNABLE PARYLENE-C SUPERHYDROPHOBIC FILMS WITH HIGH AND LOW ADHESION

Bo Lu<sup>1</sup>, Jeffrey Chun-Hui Lin<sup>1</sup>, Zhao Liu<sup>1</sup>, Yi-Kuen Lee<sup>2</sup> and Yu-Chong Tai<sup>1</sup>

<sup>1</sup>California Institute of Technology, Pasadena, California, USA

<sup>2</sup>The Hong Kong University of Science and Technology, Hong Kong, China

## ABSTRACT

This paper reports the first parylene-C based superhydrophobic films with high or low adhesion for potential droplet-based microfluidics. By creating hierarchical dual-scale micro/nanostructures and applying various plasma treatments, both biomimetic designs of lotus leaf effect with high contact angle and low adhesion, and petal effect with high contact angle but high adhesion, are demonstrated. Due to parylene's properties, these superhydrophobic films are highly flexible and transparent. Moreover, selective patterning of hydrophilic and superhydrophobic areas on a single film is also achieved. The combination of flexibility, transparency, selective patterning and simple fabrication makes our superhydrophobic films compare favorably to other designs.

## INTRODUCTION

Micromachined superhydrophobic solid surfaces have been attracting increasingly more interests in biomimetic designs and droplet-based microfluidics. In general, superhydrophobic surfaces with static contact angle (CA) larger than 150° can be divided into two categories [1]: superhydrophobic surfaces with low adhesion, which mimic lotus leaf effect, and superhydrophobic surfaces with high adhesion, which mimic rose petal effect. Both designs have numerous applications. For examples, surfaces with lotus effect have self-cleaning features and can be adopted in low-friction fluid flow [2]. Surfaces with petal effect can be used in the transport of liquid microdroplets over a surface without rolling and sliding, and used inside the aircraft ceiling to prevent the falling of condensed water droplets onto passengers [2]. While many effects have been devoted to the design of hydrophobic surfaces with lotus effect [1-5], only a few attempts were made to fabricate surfaces with petal effect [1,2].

Among various methods of creating the superhydrophobic surfaces, hierarchical dual-scale micro/nanostructure design is an effective way to achieve superhydrophobicity. To obtain the hierarchical structures, physical [6], chemical [1] and biological [4] methods have been reported. However, some of these methods require complicated multi-step operations to form the desired micro/nanostructures. In addition, most of these superhydrophobic surfaces are fabricated on rigid silicon or thick plastic substrates [1,2,4,6], which lack flexibility and prevent transferring of these designs to surfaces with curvatures. Another disadvantage of silicon or thick plastic substrates is that these superhydrophobic surfaces are opaque [1-6]. However, transparency is clearly desirable if we want to implement the superhydrophobic surfaces to goggles or

windshields [7]. Unfortunately, only a few works have explored the possibility of creating transparent superhydrophobic films due to the difficulties in material selection and fabrication [7].

Since the wettability of the solid surface also greatly depends on the surface energy, in some superhydrophobic designs, Teflon [7] or hydrophobic silane coatings [4] are needed to increase the CA, which are very difficult to further pattern. However, in some applications, such as open-channel microfluidics [8], selective patterning of hydrophilic and superhydrophobic areas onto one single surface is desirable.

In this work, by creating dual-scale micro/nanostructures on parylene-C film with different plasma treatments, we present simple methods of fabricating both types of superhydrophobic films with high and low adhesion. Due to parylene's natural properties, these superhydrophobic films are highly flexible and transparent, which are advantageous over traditional silicon or thick plastic based designs. Moreover, since the surface properties of parylene can be easily modified by plasma treatment through standard microfabrication processes, we also demonstrate the selective patterning of hydrophilic and superhydrophobic areas on a single film.

## FABRICATION

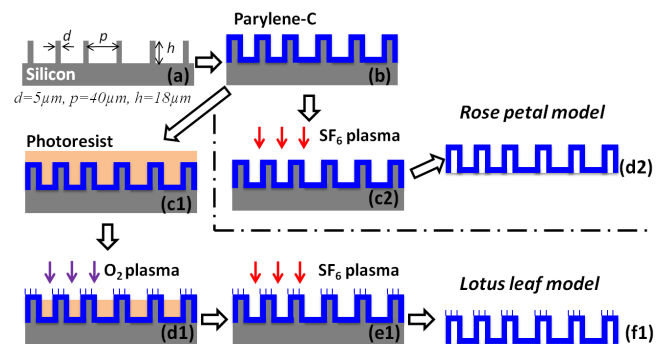


Figure 1: Fabrication process of two types of superhydrophobic parylene-C films.

The fabrication of superhydrophobic films started with DRIE etching of micropillar arrays on a silicon substrate (Fig. 1). After HMDS coating to reduce the adhesion between silicon and parylene-C, the substrate was coated with a 7 $\mu\text{m}$  thick parylene-C. For both the lotus leaf and rose petal models,  $\text{SF}_6$  plasma was used to fluorinate the parylene-C surface and increase its hydrophobicity as shown in Fig. 1 e1&c2, respectively. However, to achieve lotus effect, before  $\text{SF}_6$  plasma fluorination, ~21 $\mu\text{m}$  thick

photoresist was spin-coated on the substrate and an additional O<sub>2</sub> plasma etching step was needed to further roughen the top surface of parylene micropillars (Fig. 1 c1&d1). Finally, parylene-C films with hierarchical structures were peeled off from the silicon substrate.

## CHARACTERIZATIONS

### Fluorine Plasma Treatment

As-deposited parylene-C has a CA of around 80°. It was reported that CF<sub>4</sub> plasma can lower the surface energy and further increase the CA of parylene-C [9]. Here, the effects of surface treatments on unpatterned parylene-C films with different fluorine plasmas, including SF<sub>6</sub>, CF<sub>4</sub> and NF<sub>3</sub> plasma (300W, 300mTorr), were examined by measuring the CAs, as shown in Fig. 2a. SF<sub>6</sub> plasma was found to be the best choice, which could increase the CA of unpatterned parylene-C from ~80° to >120° within 5 minutes (Fig. 2a). For parylene-C films with micropillars, several designs with different dimensions were compared. However, at least in the range we studied, no clear difference was observed on the CA (Fig. 2b). After SF<sub>6</sub> plasma treatment, the CA of the structured parylene-C surface was enhanced to >150° (Fig. 2b), achieving superhydrophobicity. By comparing the CAs right after treatment and two months after treatment, we found that the effect of SF<sub>6</sub> plasma treatment on the hydrophobicity of parylene-C was permanent (Fig. 2c).

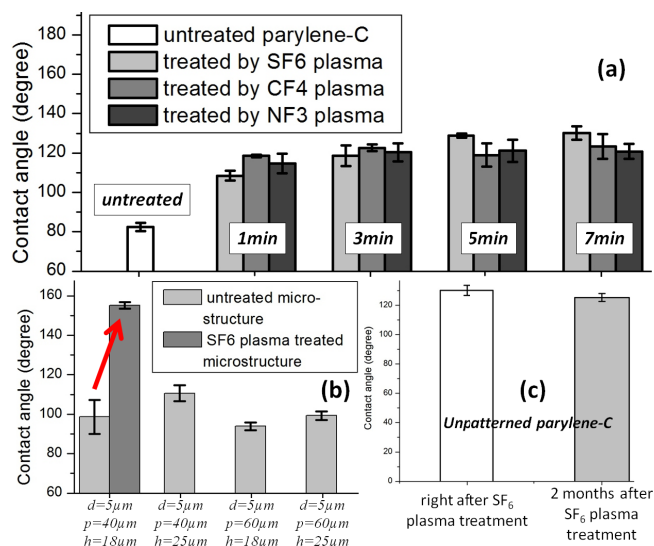


Figure 2: The effects of fluorine plasma treatment on (a) unpatterned parylene-C, and (b) structured parylene-C with micropillars. (c) Evaluation of the long-term effect of SF<sub>6</sub> plasma treatment.

### AFM Surface Roughness Evaluation

Fig. 3 shows the AFM (Veeco Instruments Inc.) measurement of parylene-C's root mean square (rms) surface roughness ( $\sigma$ ) after plasma treatments. O<sub>2</sub> plasma (300W, 300mTorr) effectively roughened parylene-C ( $\sigma > 100$ nm), especially when photoresist was pre-coated as an etching mask and was over-etched through during O<sub>2</sub> plasma treatment. However, fluorine plasma only caused slight or

moderate surface roughness ( $\sigma < 50$ nm). Fig. 3b indicates that after O<sub>2</sub> plasma roughening, nanostructures appeared on parylene surface.

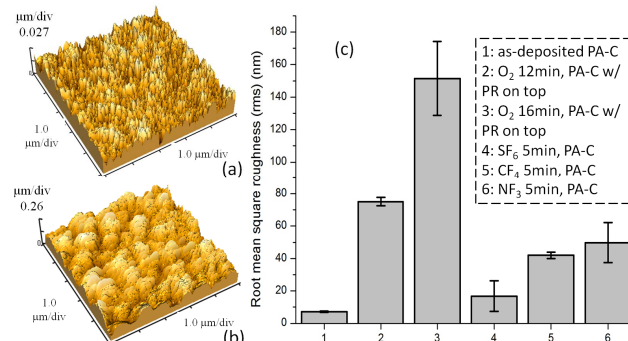


Figure 3: AFM evaluation of the rms surface roughness. (a) Untreated parylene-C (PA-C). (b) Parylene-C treated with O<sub>2</sub> plasma for 12min, with photoresist (PR) on top. (c) Rms roughness of Parylene-C with different plasma treatment conditions.

### SEM Observations

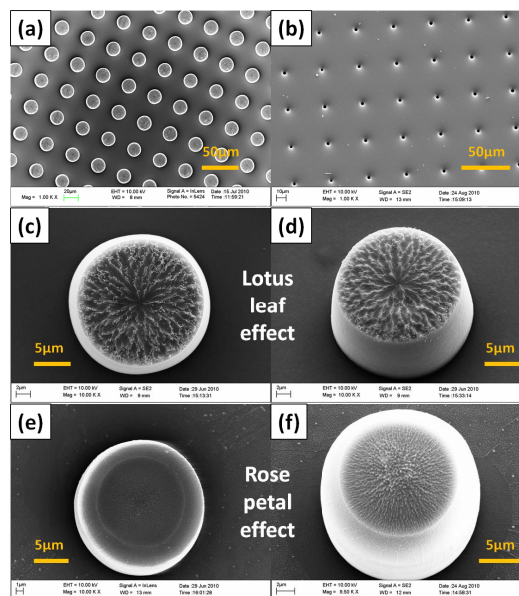


Figure 4: SEM images of (a)&(b) top view of the front and back sides of the superhydrophobic film. (c)&(d) top and tilted views of superhydrophobic structure which mimics lotus leaf. (e)&(f) top and tilted views of superhydrophobic structure which mimics rose petal.

Fig. 4 a&b show the SEM (Zeiss 1550 VP FESEM) images of the front and backside of the fabricated superhydrophobic film. Since parylene is mechanically robust but flexible, no damage was observed after peeling off the film from the silicon substrate. Corresponding to the AFM results, SEM images show that the lotus leaf model has highly-roughened nanostructures on the top surface of micropillars due to O<sub>2</sub> plasma (Fig. 4 c&d). In comparison, for rose petal model, the micropillar has a much smoother top surface (Fig. 4 e&f), with only small nanostructures.

## EXPERIMENTAL RESULTS

### Superhydrophobic Film with Low Adhesion

To evaluate the CA and contact angle hysteresis (CAH) of the superhydrophobic film with low adhesion, a deionized water droplet of 4  $\mu\text{L}$  volume was dispensed by a micropipette on the top surface, and the CA was measured with a Contact Angle Goniometer (Model 100-00, ramé-hart instrument co.). The CAH is defined as the difference between the advancing and receding angles, which were measured by increasing or decreasing the volume of the water droplet while keeping the bottom contact area unchanged. Water droplet had a CA of  $155.5 \pm 3.7^\circ$  on this hierarchical structure, and there were clear trapped air pockets (Fig. 5a). The low adhesion between the droplet and film was demonstrated by measuring the advancing and receding angles (Fig. 5 b&c), and a low CAH of  $\sim 6^\circ$  was calculated. All the images were taken with an eyepiece camera mounted onto the Goniometer.

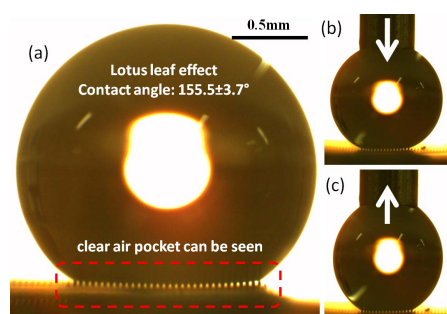


Figure 5: Water droplet on a superhydrophobic film with low adhesion (lotus leaf). (a) CA measurement. A clear air pocket was observed. (b) Advancing angle. (c) Receding angle.

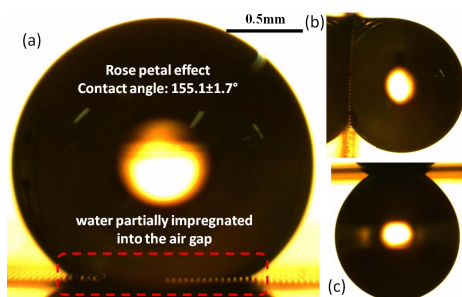


Figure 6: Water droplet on a superhydrophobic film with high adhesion (rose petal). (a) CA measurement. Water partially impregnated the gap; (b)&(c) droplet stayed on the film when tilted for  $90^\circ$  and  $180^\circ$ .

### Superhydrophobic Film with High Adhesion

In the case of a superhydrophobic film with high adhesion, the CA was measured to be  $155.1 \pm 1.7^\circ$  (Fig. 6a). However, unlike the low adhesion case, water could partially impregnate the microstructures, resulting in a not well-defined air pocket. To demonstrate the high adhesion which was probably ascribed to the penetrated water, the superhydrophobic film was tilted for  $90^\circ$  and  $180^\circ$ . The

droplet still adhered to the surface when placed vertically or turned upside down (Fig. 6 b&c).

### Theoretical Explanations

In general, a droplet in contact with microstructured surfaces can be divided into two types of wetting states [10]. As shown in Fig. 7a, if the liquid is in intimate contact with the solid structures, the droplet is in the Wenzel state. In contrast, if the liquid rests on the top of the structures, it is in the Cassie state. However, for hierarchical dual-scale micro/nanostructures, the wetting states on microscale and nanoscale may be different [6]. Hence, mixed wetting states should be introduced to explain the difference between superhydrophobic surfaces with high and low adhesions. For the lotus leaf model, since the nanostructures on top of the micropillars are highly rough, both of the water-micropillars and water-nanopatterns interactions are likely in the non-wetting Cassie-Cassie state (Fig. 7b). On the contrary, since the rose petal model has much smoother nanotextures on top of the micropillars, water can wet these small nanoscale textures, and partially impregnates between the microstructures, which could be described by a mixed Cassie-Wenzel state (Fig. 7b).

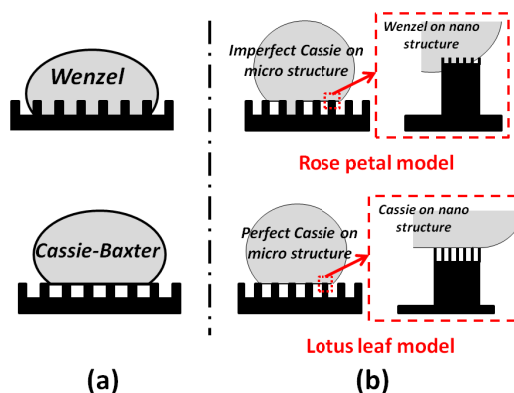


Figure 7: Theoretical models showing different wetting states on structured surfaces. (a) Classic Wenzel and Cassie-Baxter states. (b) Mixed Cassie-Wenzel and non-wetting Cassie-Cassie states describing droplets resting on hierarchical micro/nanostructures.

## DISCUSSION

Flexibility becomes an outstanding feature when curved, folded or 3D superhydrophobic films are desirable [5,7]. Compared with the other designs on rigid or thick substrates [1,2,4,6], our superhydrophobic thin film could be easily transferred to a curved metal rod (Fig. 8).

The optical transmittance and absorptance of as-deposited parylene-C, parylene-C with micropillars only, and parylene-C with hierarchical patterns were measured with an 8453 UV-Visible spectrophotometer (Agilent Technologies). Fig. 9 demonstrates the transparency of the superhydrophobic film, showing unique advantage over silicon or thick plastic based designs [1-6]. Although the micro and nanopatterns reduced the transmittance by



10-25%, the film was still transparent as shown in Fig. 9b. Words underneath the superhydrophobic film could be clearly seen.

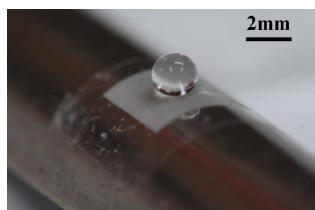


Figure 8: Demonstration of the flexibility of our superhydrophobic film.

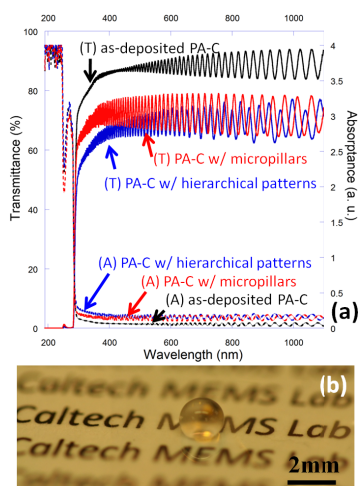


Figure 9: Transparency of the superhydrophobic film. (a) Optical transmittance and absorbance. (b) A demonstration of the high transparency.

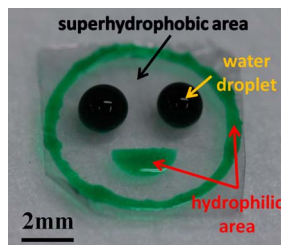


Figure 10: Demonstration of the selective patterning of hydrophilic and superhydrophobic areas.

Unlike Teflon [7] or hydrophobic silane-coated [4] surfaces which are difficult to pattern, we proved the selective patterning of hydrophilic and superhydrophobic areas on a single film (Fig. 10). The hydrophilic areas (the mouth and the outline of the face) were treated with oxygen plasma, having a CA  $\sim 5^\circ$ . The surface fluid was confined within these hydrophilic areas. The other areas were superhydrophobic with CA  $\sim 155^\circ$ . The eyes were two near-spherical droplets. Deionized water was labeled by food dye. Photoresist was used as mask for the selective patterning.

## CONCLUSION

In this paper, we propose simple methods of creating novel superhydrophobic parylene-C films with high and low adhesions for the biomimetic designs of both lotus leaf and rose petal. The combination of flexibility, transparency, selective patterning and simple fabrication makes our superhydrophobic films compare favorably to other designs.

## ACKNOWLEDGEMENT

The authors would like to thank Mr. Alex Miller from Chemistry Department of Caltech for his help with the UV-Vis Spectroscopy.

## REFERENCES

- [1] S. Zhu, Y. Li, J. Zhang, C. Lu, X. Dai, F. Jia, H. Gao and B. Yang, "Biomimetic polyimide nanotube arrays with slippery or sticky superhydrophobicity", *J. Colloid Interface Sci.*, vol. 344, pp. 541-546, 2010.
- [2] B. Bhushan and E. K. Her, "Fabrication of superhydrophobic surfaces with high and low adhesion inspired from rose petal", *Langmuir*, vol. 26, pp. 8207-8217, 2010.
- [3] M. Im, D. H. Kim, X. J. Huang, J. H. Lee, J. B. Yoon and Y. K. Choi, "A highly flexible superhydrophobic microlens array with small contact angle hysteresis for droplet-based microfluidics", *Proc. of MEMS 2009*, Sorrento, Italy, 2009, pp. 475-478.
- [4] M. McCarthy, R. Enright, K. Gerasopoulos, J. N. Culver, R. Ghodssi and E. N. Wang, "Biomimetic superhydrophobic surfaces using viral nanotemplates for self-cleaning and dropwise condensation", *Proc. of Hilton Head 2010*, Hilton Head Island, SC, USA, 2010, pp. 86-89.
- [5] M. Xu, N. Lu, H. Xu, D. Qi, Y. Wang, S. Shi and L. Chi, "Fabrication of flexible superhydrophobic biomimic surfaces", *Soft Matter*, vol. 6, pp. 1438-1443, 2010.
- [6] T. G. Cha, J. W. Yi, M. W. Moon, K. R. Lee and H. Y. Kim, "Nanoscale patterning of microtextured surfaces to control superhydrophobic robustness", *Langmuir*, vol. 26, pp. 8319-8326, 2010.
- [7] M. Im, H. Im, J. H. Lee, J. B. Yoon and Y. K. Choi, "A robust superhydrophobic and superoleophobic surface with inverse-trapezoidal microstructures on a large transparent flexible substrate", *Soft Matter*, vol. 6, pp. 1401-1404, 2010.
- [8] Y. Zhou, C. Qian, W. Wang and W. Wu, "Parylene based two-dimensional open microfluidic channels", *Proc. of  $\mu$ TAS 2009*, Jeju, Korea, 2009, pp. 884-886.
- [9] Y. H. Ham, D. A. Shutov, K. H. Baek, L. M. Do, K. Kim, C. W. Lee and K. H. Kwon, "Surface characteristics of parylene-C films in an inductively coupled  $O_2/CF_4$  gas plasma", *Thin Solid Films*, vol. 518, pp. 6378-6381, 2010.
- [10] A. H. Cannon and W. P. King, "Curvature affects superhydrophobicity on flexible silicone microstructured surfaces", *Proc. of Transducers 2009*, Denver, CO, USA, 2009, pp. 362-365.